Hydrothermal Synthesis and Structural Characterisation of $SrFe_3(PO_4)_3(HPO_4)$, an Iron(III) Phosphate containing FeO_5 Trigonal Bipyramids and Dimers of Face-sharing FeO_6 Octahedra *

Kwang-Hwa Lii,[a] Teng-Yuan Dong,[a] Chih-Yi Cheng[b] and Sue-Lein Wang[b]
[a] *Institute of Chemistry, Academia Sinica, Taipei, Taiwan, Republic of China*
[b] *Department of Chemistry, National Tsing Hua University, Hsinchu, Taiwan, Republic of China*

A new iron(III) phosphate, $SrFe_3(PO_4)_3(HPO_4)$, has been synthesised hydrothermally and characterised by single-crystal X-ray diffraction and Mössbauer spectroscopy. The compound crystallises in the monoclinic space group $P2_1/c$, with $a = 8.476(2)$, $b = 7.298(1)$, $c = 19.501(3)$ Å, $\beta = 94.96(2)°$, and $Z = 4$. The structure consists of channels parallel to the a axis where the Sr atoms are located. The framework is composed of dimers of face-sharing FeO_6 octahedra, discrete FeO_5 trigonal bipyramids, phosphate tetrahedra, and hydrogenphosphate groups. Room-temperature Mössbauer spectroscopy confirms the presence of high-spin Fe^{III}.

Recently we have found a number of new structures in the ternary vanadium phosphate system using hydrothermal techniques under acidic conditions. Compounds such as $K_2(VO)_3(HPO_4)_4$,[1] β-$LiVOPO_4$,[2] $Ca(VO)_2(PO_4)_2$,[3] $A(VOPO_4)_2 \cdot nH_2O$ (A = Na, K, Rb, Ca, Sr, Pb, Co or Ni; n = 3 or 4),[4,5] $Ca_2V(PO_4)(HPO_4)_2 \cdot H_2O$,[6] $Ca_2V(PO_4)(P_2O_7)$[6] and AVO_2PO_4 (A = Sr or Ba)[7] have been isolated. These phosphates adopt tunnel or layer structures with the ternary metal cations located in sites within the tunnels or between the layers.

Iron phosphates are significant in corrosion inhibition, passivation of metal surfaces[8] and heterogeneous catalysis,[9,10] and present a variety of complex network structures. Basic and/or hydrated iron phosphates exist as minerals and are considered as among the most perplexing substances in the mineral kingdom.[11] With ternary compounds, most are either anhydrous alkali-metal iron phosphates and oxyphosphates, or basic and/or hydrated alkaline-earth metal iron phosphates. It appears that the synthesis of alkaline-earth metal iron phosphates under acidic conditions would be interesting. Since hydrothermal techniques proved to be particularly suitable for the synthesis of low-temperature phases and useful for crystal growth, we have extended our research aimed at synthesising ternary iron phosphate crystals from phosphoric acid solutions under hydrothermal conditions. This paper reports the hydrothermal synthesis, crystal structure determination, and Mössbauer spectroscopy study of a new strontium iron(III) phosphate, $SrFe_3(PO_4)_3(HPO_4)$.

Experimental

Synthesis.—Reagent grade $Sr(OH)_2 \cdot 8H_2O$, $FePO_4$ and 85% H_3PO_4, obtained from Merck, were used as received. Crystals of $SrFe_3(PO_4)_3(HPO_4)$ were grown by heating a mixture of $Sr(OH)_2 \cdot 8H_2O$ (0.1512 g), $FePO_4$ (0.2574 g) (molar ratio Sr:Fe = 1:3), and of 3.75 mol dm^{-3} H_3PO_4 (2.0 cm^3) in a sealed quartz glass tube (inside diameter 8 mm, outside diameter 10 mm) at 400 °C for 48 h followed by slow cooling at 40 °C h^{-1} to room temperature. The glass tube was ≈50% filled including the volume of the undissolved solid. The glass tube was heated in a pressure vessel in which the pressure inside the glass tube was balanced by an external pressure to keep the tube intact. Visual microscopic examination showed that the product contained many tan prisms of the required compound along with some colourless unidentified polycrystalline material. A single-phase product was not obtained, although several different reaction conditions were tested. Subsequently, a reaction was performed in a gold-lined Morey-type closure autoclave (17.5 cm × 3.3 cm inside diameter) with an internal volume of 140 cm^3. A reaction mixture of $FePO_4$ (10.846 g), $Sr(OH)_2 \cdot 8H_2O$ (6.370 g) (molar ratio Sr:Fe = 1:3), and 3.75 mol dm^{-3} H_3PO_4(aq) (70 cm^3) was heated at 400 °C for 4 d followed by cooling to room temperature in 5 h. Upon opening the autoclave the product was found to contain many tan crystals of several mm in length and some colourless crystals of low quality. Energy-dispersive X-ray fluorescence analysis on a tan crystal showed that the Sr:Fe:P mole ratio was 1:2.99:4.10. Powder X-ray diffraction and elemental analysis using a Rigaku powder diffractometer and an ICP-AE spectrometer, respectively, on a sample of manually selected tan crystals confirmed their purity for subsequent Mössbauer spectroscopy study (Found: Fe, 26.4; P, 19.5; Sr, 13.9. Calc. for $SrFe_3(PO_4)_3(HPO_4)$: Fe, 26.35; P, 19.50; Sr, 13.75%).

Single-crystal X-Ray Diffraction.—A tan crystal having dimensions of 0.20 × 0.28 × 0.50 mm was selected for indexing and intensity data collection on a Nicolet R3m/V diffractometer with graphite-monochromated Mo-Kα radiation. Unit-cell parameters and the orientation matrix were determined by a least-squares fit of 15 peak maxima with 2θ ranging from 10 to 29°. Axial oscillation photographs were taken to check the unit-cell parameters and symmetry properties. Of the 3172 reflections collected ($2\theta_{max} = 55°$), 2295 unique reflections were considered observed [$I > 3.0\sigma(I)$] after Lorentz polarisation and empirical absorption corrections. Correction for absorption was based on ψ scans of a few suitable reflections with χ values close to 90° using the program XEMP of the SHELXTL PLUS program package.[12] Based on the systematic absences and successful solution and refinement of the structure, the space group was determined to be $P2_1/c$. Direct methods (SHELXTL PLUS) were used to locate the metal atoms with the remaining non-hydrogen atoms being found from successive difference

* *Supplementary data available:* see Instructions for Authors, *J. Chem. Soc., Dalton Trans.*, 1993, Issue 1, pp. xxiii–xxviii.

Table 1 Crystal data and intensity collection parameters for $SrFe_3(PO_4)_3(HPO_4)$

Formula	$SrFe_3(PO_4)_3(HPO_4)$
M	636.1
Crystal symmetry	Monoclinic
Space group	$P2_1/c$
a/Å	8.476(2)
b/Å	7.298(1)
c/Å	19.501(3)
β/°	94.96(2)
U/Å^3	1201.8(4)
Z	4
D_c/g cm^{-3}	3.515
$F(000)$	1220
μ(Mo-Kα)/cm^{-1}	84.59
T/°C	24
Scan rate/° min^{-1}	Variable; 2.93–14.65° min^{-1} in ω
Scan mode	θ–2θ
Scan width/°	1.00° plus Kα separation
2θ range/°	2–55
No. of reflections collected	3172
Unique obs. reflections [$I > 3\sigma(I)$]	2295
Refined parameters	222
R^a	0.0261
R'^b	0.0276

^{a} $R = \Sigma||F_o| - |F_c||/\Sigma|F_o|$. ^{b} $R' = [\Sigma w(|F_o| - |F_c|)^2/\Sigma wF_o^2]^{\frac{1}{2}}$.

Table 2 Positional parameters for $SrFe_3(PO_4)_3(HPO_4)$

Atom	x	y	z
Sr	0.202 33(4)	0.063 55(5)	0.562 42(2)
Fe(1)	−0.217 29(6)	0.434 37(7)	0.418 06(3)
Fe(2)	−0.270 20(6)	−0.006 54(7)	0.214 00(3)
Fe(3)	0.263 86(6)	−0.102 71(7)	0.309 04(3)
P(1)	0.447 3(1)	0.206 8(1)	0.399 24(5)
P(2)	−0.384 9(1)	−0.317 4(1)	0.310 51(5)
P(3)	−0.015 4(1)	0.206 2(1)	0.318 03(5)
P(4)	−0.114 3(1)	0.318 8(1)	0.568 24(5)
O(1)	−0.052 7(3)	0.616 9(4)	0.405 7(1)
O(2)	−0.190 0(3)	0.462 3(4)	0.516 1(1)
O(3)	−0.098 0(3)	0.234 2(4)	0.384 7(1)
O(4)	−0.360 6(3)	0.631 5(4)	0.388 1(1)
O(5)	−0.380 7(3)	0.231 1(4)	0.428 0(2)
O(6)	−0.147 5(3)	0.200 1(4)	0.258 1(1)
O(7)	−0.222 2(3)	0.187 5(3)	0.127 8(1)
O(8)	−0.436 9(3)	0.195 9(4)	0.212 8(1)
O(9)	−0.407 9(3)	−0.154 7(4)	0.156 8(2)
O(10)	−0.089 6(3)	−0.132 9(4)	0.193 4(1)
O(11)	−0.307 4(3)	−0.128 4(4)	0.302 0(1)
O(12)	0.306 7(3)	0.033 6(4)	0.228 8(2)
O(13)	0.418 4(3)	0.009 9(4)	0.376 6(2)
O(14)	0.071 3(3)	0.023 4(4)	0.325 1(1)
O(15)	0.335 8(4)	0.237 9(4)	0.459 4(2)
H(15)	0.281(7)	0.351(7)	0.463(3)
O(16)	−0.097 9(3)	0.135 3(4)	0.533 5(1)

maps. Bond-strength calculations were carried out to help locate any hydrogen atoms. One oxygen atom was found to be considerably undersaturated; a valence sum of 1.30 was calculated for O(15). This value suggests that O(15) is bonded to a hydrogen atom. The hydrogen atom was located from a difference map. Subsequent refinement, including the atomic coordinates and anisotropic thermal parameters for all non-hydrogen atoms and an isotropic thermal parameter for the hydrogen atom, converged at $R = 0.0261$ and $R' = 0.0276$ $\{w = 1/[\sigma^2(F) + 0.000\,567F^2]\}$. The occupancy factor of Sr was allowed to refine but did not deviate significantly from full occupancy. Therefore, the strontium metal site was considered fully occupied in the final cycles of refinement. Neutral-atom scattering factors for all atoms were taken from ref. 13. Anomalous dispersion corrections were applied.

Table 3 Selected bond lengths (Å) and bond valence sums (Σs) for $SrFe_3(PO_4)_3(HPO_4)$

Sr–O(1)	2.751(3)	Sr–O(3)	2.593(3)
Sr–O(4)	2.731(3)	Sr–O(5)	2.626(3)
Sr–O(11)	2.756(3)	Sr–O(15)	2.707(3)
Sr–O(16)	2.470(3)	Sr–O(16)	2.611(3)
Σs(Sr–O) = 1.93			
Fe(1)–O(1)	1.959(3)	Fe(1)–O(2)	1.916(3)
Fe(1)–O(3)	1.922(3)	Fe(1)–O(4)	1.940(3)
Fe(1)–O(5)	2.050(3)		
Σs[Fe(1)–O] = 2.95			
Fe(2)–O(6)	1.984(3)	Fe(2)–O(7)	2.262(3)
Fe(2)–O(8)	2.043(3)	Fe(2)–O(9)	1.884(3)
Fe(2)–O(10)	1.861(3)	Fe(2)–O(11)	1.983(3)
Σs[Fe(2)–O] = 3.28			
Fe(3)–O(12)	1.915(3)	Fe(3)–O(13)	1.956(3)
Fe(3)–O(14)	1.923(4)	Fe(3)–O(6)	2.129(3)
Fe(3)–O(7)	2.015(3)	Fe(3)–O(8)	2.145(3)
Σs[Fe(3)–O] = 3.11			
P(1)–O(13)	1.517(3)	P(1)–O(15)	1.584(3)
P(1)–O(5)	1.526(3)	P(1)–O(9)	1.505(3)
Σs[P(1)–O] = 5.04			
P(2)–O(11)	1.543(3)	P(2)–O(4)	1.554(3)
P(2)–O(8)	1.542(3)	P(2)–O(12)	1.516(3)
Σs[P(2)–O] = 4.95			
P(3)–O(3)	1.543(3)	P(3)–O(6)	1.548(3)
P(3)–O(14)	1.524(3)	P(3)–O(10)	1.501(3)
Σs[P(3)–O] = 5.08			
P(4)–O(2)	1.559(3)	P(4)–O(16)	1.513(3)
P(4)–O(1)	1.536(3)	P(4)–O(7)	1.540(7)
Σs[P(4)–O] = 4.97			

Additional material available from the Cambridge Crystallographic Data Centre comprises thermal parameters and remaining bond lengths and angles.

Mössbauer Spectroscopy.—The ^{57}Fe Mössbauer measurements were made on a constant-acceleration instrument as reported elsewhere.[14] Velocity calibrations were made using 99.99% pure 10-μm iron foil. Typical linewidths for all three pairs of iron lines fell in the range 0.28–0.30 mm s^{-1}. Isomer shifts are reported with respect to iron foil at 300 K. It should be noted that the isomer shifts illustrated are plotted as experimentally obtained; tabulated data should be consulted.

Results and Discussion

Structural Description.—The crystallographic data are listed in Table 1, atomic coordinates in Table 2 and selected bond distances and bond valence sums[15] in Table 3. All atoms are located on general positions. The iron atoms are both five- and six-co-ordinated. The co-ordination number of Sr^{2+} was determined on the basis of the maximum gap in the Sr–O distances ranked in increasing order. It is co-ordinated by eight oxygen atoms and the ninth Sr–O bond length is at 3.373 Å. Bond valence sums for the Sr, Fe(1), Fe(3) and P atoms are in good accordance with their formal oxidation states. The value of Fe(2) is somewhat higher.

As shown in Fig. 1, the $SrFe_3(PO_4)_3(HPO_4)$ structure consists of channels down the a axis where the Sr atoms are located. The framework is composed of Fe_2O_9 units formed by two face-sharing FeO_6 octahedra, discrete FeO_5 trigonal bipyramids, phosphate tetrahedra, and hydrogenphosphate groups. The Fe_2O_9 units are interconnected by PO_4 and HPO_4 groups to form sheets in the ab plane as shown in Fig. 2. The trigonal bipyramids connect the sheets into a three-dimensional framework. Dimers of face-sharing FeO_6 octahedra have also been observed in $Fe_4(OH)_3(PO_4)_3$[16] and $Fe_2(P_2O_7)(HPO_4)$.[17] The latter compound consists of similar sheets of interconnected Fe_2O_9 and HPO_4 units. Five-co-ordination with trigonal-bipyramidal geometry is frequently found in iron phosphates.

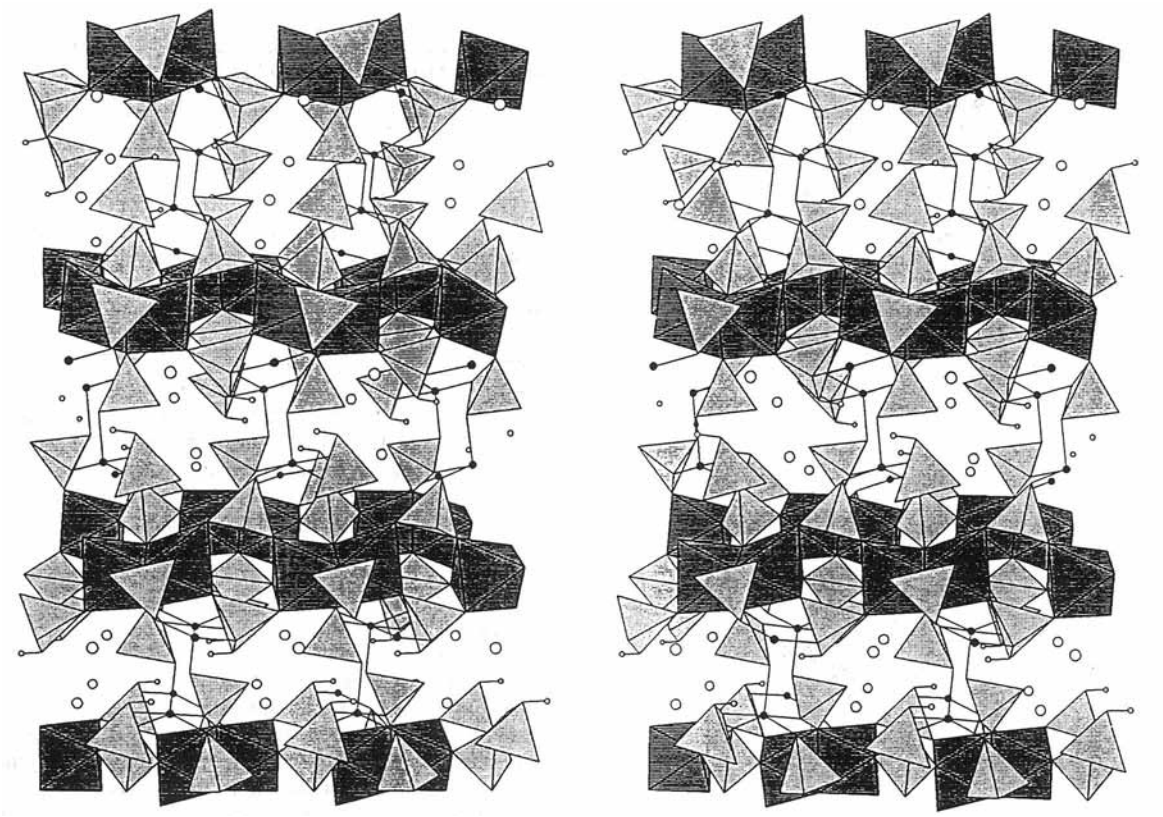

Fig. 1 Stereoscopic view of the $SrFe_3(PO_4)_3(HPO_4)$ structure along the [100] direction. In this representation the corners of octahedra and tetrahedra are O atoms and the Fe and P atoms are at the centre of each octahedron and tetrahedron, respectively. Small open circles, H atoms; large open circles, Sr atoms; solid circles, Fe(1) atoms

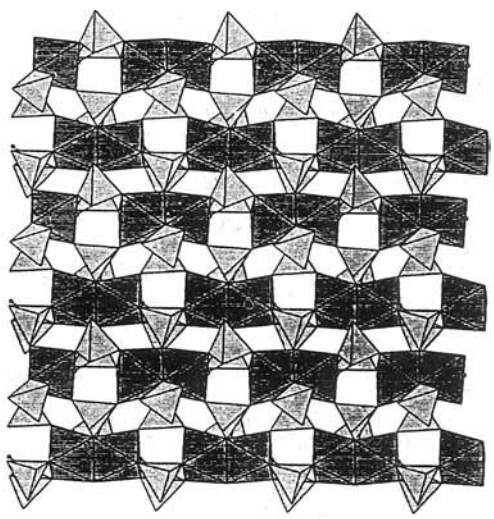

Fig. 2 Section of a sheet of interconnected Fe_2O_9, PO_4 and HPO_4 units in $SrFe_3(PO_4)_3(HPO_4)$ along the [001] direction

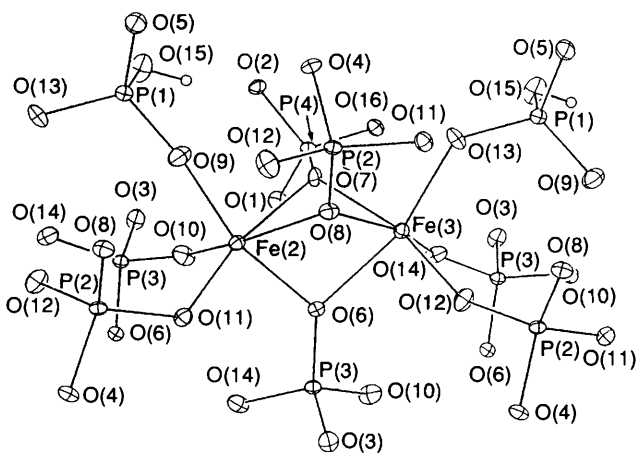

Fig. 3 The co-ordination of phosphate ligands around a dimer of face-sharing FeO_6 octahedra in $SrFe_3(PO_4)_3(HPO_4)$

The nine vertices of each dimer in the present compound are shared with 2 HPO_4 groups and 7 PO_4 tetrahedra (Fig. 3). As shown by the O ··· O distances 2.535–3.083 Å for $Fe(2)O_6$ and 2.535–3.026 Å for $Fe(3)O_6$, both octahedra are strongly distorted. The common edges of the two FeO_6 octahedra are 2.535–2.566 Å and are considerably shorter than those of edges which are not shared. The iron ions are displaced from the centroids of their FeO_6 octahedra away from each other such that the Fe ··· Fe separation is increased from 2.427 to 2.982 Å, indicative of the absence of iron–iron bonding. The shortening of the shared edges is an evidence that the structure is predominantly ionic. The average Fe(2)–O and Fe(3)–O distances are 2.003 and 2.014 Å, respectively. The octahedral distortion can be estimated by using the equation $\Delta = (1/6)\Sigma[(R_i - \bar{R})/\bar{R}]^2$, where R_i = individual bond length and $\bar{R}$ = average bond length.[18] The calculation results show that $Fe(2)O_6$ ($10^4 \times \Delta = 43$) is more distorted than $Fe(3)O_6$ ($10^4 \times \Delta = 34$). As shown in Fig. 4, each Fe(1) atom is co-ordinated to one HPO_4 and four PO_4 groups in a distorted trigonal bipyramid with an average Fe–O distance of 1.957 Å and distorted bond angles and O ··· O distances. The axial Fe(1)–O bonds (1.959, 2.050 Å) are longer than the equatorial (1.916–1.940 Å). The Fe atom and three equatorial O atoms are very nearly coplanar.

Each of the four unique phosphorus atoms is within a somewhat distorted tetrahedron. All oxygen atoms in the phosphate groups except O(15) and O(16) bridge a phosphorus atom to one or two iron atoms. Atom O(16) is bonded to two Sr

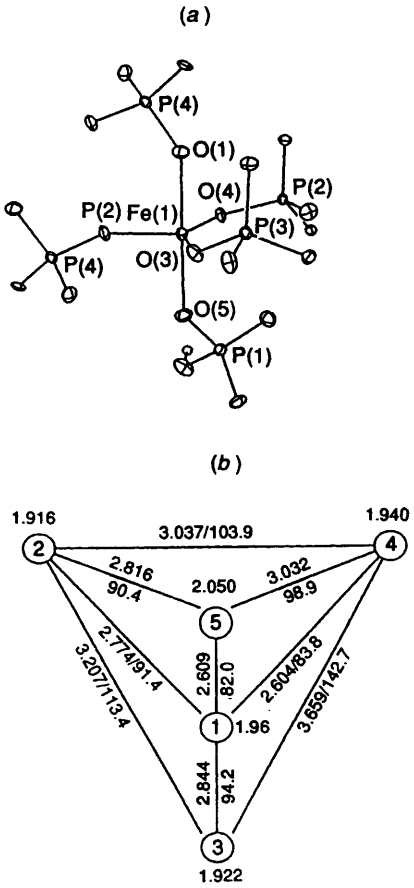

Fig. 4 (*a*) The co-ordination of phosphate ligands around a FeO_5 trigonal bipyramid in $SrFe_3(PO_4)_3(HPO_4)$. (*b*) Schlegel projection of a FeO_5 trigonal bipyramid. The central Fe atom is not included in the projection. The Fe–O distances (Å) are given at the terminal positions of the projection. The O • • • O distances and their corresponding angles (°) with respect to the central atom are indicated next to the edges

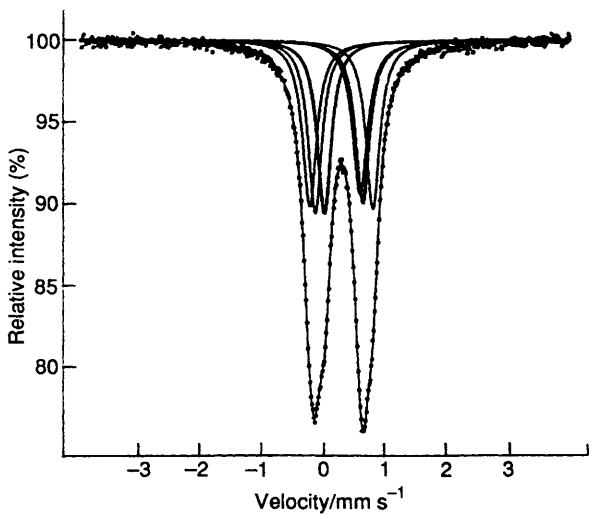

Fig. 5 Mössbauer spectrum of $SrFe_3(PO_4)_3(HPO_4)$ at 300 K

atoms, and O(15) to one H and one Sr. Not surprisingly, the P(1)–O(15) distance is the longest P–O distance in the structure.

Mössbauer Spectra.—The room-temperature Mössbauer spectrum (Fig. 5) can be described by the overlap of three symmetric doublets with equal intensities. The results presented in Table 4 are typical of paramagnetic high-spin iron(III). Based on the room-temperature Mössbauer data compiled by Gleitzer,[19] the doublets with $\delta = 0.41$ and 0.43 mm s^{-1} are assigned to two octahedral Fe atoms, and the doublet with $\delta = 0.37$ mm s^{-1} to the trigonal-bipyramidal Fe atom. The linewidths after deconvolution are ≈ 0.28 mm s^{-1}, close to that obtained for a thin iron calibration foil. The octahedral Fe atoms have very different quadrupole splittings because their deviations from perfect octahedral symmetry are somewhat different. The octahedron around Fe(2) is more distorted and it is likely the site corresponding to the larger quadrupole splitting. The isomer shift of 0.37 mm s^{-1} is close to the room-temperature value of 0.34 mm s^{-1} for the trigonal-bipyramidal iron site in Fe_3PO_7.[20]

Table 4 Iron-57 Mössbauer least-squares fitting parameters (mm s^{-1}) for $SrFe_3(PO_4)_3(HPO_4)$ at 300 K

δ^a	ΔE_Q	Γ^b
0.37	0.79	0.29, 0.27
0.41	1.04	0.28, 0.28
0.43	0.58	0.27, 0.30

[a] Isomer shift. [b] Full width at half-height taken from the least-squares fitting program. The width for the line at more positive velocity is listed first for each doublet.

The iron phosphate system has a rich crystal chemistry and contains a large number of structure types. Their complex crystal structures and interesting magnetic properties are a challenge to characterisation. Since hydrothermal methods have been successfully used in the synthesis and crystal growth of new crystalline phases, it is likely that many more iron phosphates with novel frameworks will be forthcoming.

Acknowledgements

We are indebted to the National Science Council of the Republic of China for financial support.

References

1 K. H. Lii and H. J. Tsai, *J. Solid State Chem.*, 1991, **91**, 331.
2 K. H. Lii, C. H. Li, C. Y. Cheng and S. L. Wang, *J. Solid State Chem.*, 1991, **95**, 352.
3 K. H. Lii, B. R. Chueh, H. Y. Kang and S. L. Wang, *J. Solid State Chem.*, 1992, **99**, 72.
4 S. L. Wang, H. Y. Kang, C. Y. Cheng and K. H. Lii, *Inorg. Chem.*, 1991, **30**, 3496.
5 H. Y. Kang, W. C. Lee, S. L. Wang and K. H. Lii, *Inorg. Chem.*, 1992, **31**, 4743.
6 K. H. Lii, N. S. Wen, C. C. Su and B. R. Chueh, *Inorg. Chem.*, 1992, **31**, 439.
7 H. Y. Kang, S. L. Wang and K. H. Lii, *Acta Crystallogr., Sect. C*, 1992, **48**, 975.
8 W. Meisel, H. J. Guttmann and P. Gutlich, *Corros. Sci.*, 1983, **23**, 1373.
9 J. B. Moffat, *Catal. Rev. Sci. Eng.*, 1978, **18**, 199.
10 M. Forissier, D. Foujols, A. Modaressi and C. Gleitzer, *Bull. Soc. Chim. Fr.*, 1985, 410.
11 P. B. Moore, *Am. Mineral.*, 1970, **55**, 135.
12 G. M. Sheldrick, SHELXTL-PLUS Crystallographic Systems, release 4.11, Siemens Analytical X-Ray Instruments, Madison, WI, 1990.
13 *International Tables for X-Ray Crystallography*, Kynoch Press, Birmingham, 1974, vol. 4.
14 T. Y. Dong, C. C. Schei, T. L. Hsu, S. L. Lee and S. J. Li, *Inorg. Chem.*, 1991, **30**, 2457.
15 I. D. Brown and D. Altermatt, *Acta Crystallogr., Sect. B*, 1985, **41**, 244.
16 C. C. Torardi, W. M. Reiff and L. Takacs, *J. Solid State Chem.*, 1989, **82**, 203.
17 W. M. Reiff and C. C. Torardi, *Hyperfine Interact.*, 1990, **53**, 403.
18 R. D. Shannon, *Acta Crystallogr., Sect. A*, 1976, **32**, 751.
19 C. Gleitzer, *Eur. J. Solid State Inorg. Chem.*, 1991, **28**, 77.
20 A. Modaressi, A. Courtois, R. Gerardin, B. Malaman and C. Gleitzer, *J. Solid State Chem.*, 1983, **47**, 245.

Received 9th September 1992; *Paper* 2/04861B